arXiv:cond-mat/0502501v1 [cond-mat.mes-hall] 21 Feb 2005

Integration of a gate electrode into carbon nanotube devices for scanning tunneling microscopy

J. Kong, B.J. LeRoy, S.G. Lemay, and C. Dekker*
Kavli Institute of Nanoscience, Delft University of Technology, Lorentzweg 1, 2628 CJ Delft, The Netherlands

(Dated: February 2, 2008)

We have developed a fabrication process for incorporating a gate electrode into suspended single-walled carbon nanotube structures for scanning tunneling spectroscopy studies. The nanotubes are synthesized by chemical vapor deposition directly on a metal surface. The high temperature (800 °C) involved in the growth process poses challenging issues such as surface roughness and integrity of the structure which are addressed in this work. We demonstrate the effectiveness of the gate on the freestanding part of the nanotubes by performing tunneling spectroscopy that reveals Coulomb blockade diamonds. Our approach enables combined scanning tunneling microscopy and gated electron transport investigations of carbon nanotubes.

Single-walled carbon nanotubes (SWCNTs) have attracted tremendous attention in recent years due to their unique properties and promising applications.[1,2] In particular, their electronic properties have been under intensive study, both for interest in fundamental one-dimensional physics and for exploration of potential molecular electronic devices.[3,4] Scanning tunneling microscopy (STM) is a powerful tool for characterizing SWCNTs since the atomic and electronic structures can be obtained simultaneously for each nanotube.[5,6] However, the close proximity of a conducting substrate and the difficulty of incorporating a gate electrode[7] limits the range of phenomena that can be studied using STM. Both of these limitations can be overcome by suspending the SWCNT over a trench with a gate electrode at the bottom of the trench (Fig 1(a)). In such a device geometry, electron transport measurements can be combined with STM studies. Even without the gate electrode or separate source and drain contacts, new effects are observed using the STM over the freestanding portion of the SWCNT.[8,9] The addition of a gate electrode allows addressing a wealth of extra information such as band bending along the nanotube, the electronic structure during transport, electromechanical effect upon gating, etc.

In this Letter, we demonstrate the fabrication of a suspended SWCNT device with an integrated gate electrode for STM investigation. The conventional method of nanotube sample preparation for STM involves sonicating SWCNTs in organic solvents followed by depositing the suspension over a conducting substrate. When nanotubes are deposited over a surface with trenches we find that they usually sag over the trench (data not shown), presumably due to capillary forces upon drying of the solvent. The sagging of the SWCNT significantly hinders access to the suspended portion of the SWCNT. To overcome this difficulty, we chose to directly grow the nanotubes on a conducting surface by chemical vapor deposition (CVD). This has the additional advantage of allowing us to image the as-grown nanotubes without any post-processing. The main challenge in realizing such devices comes from the high temperature involved in the CVD process. This brings up issues such as choice of substrate material, surface roughness and device integrity. We will address these in the following and show that it is possible to realize a 3-terminal device, with the capability of gating and simultaneous atomic-resolution imaging and spectroscopy.

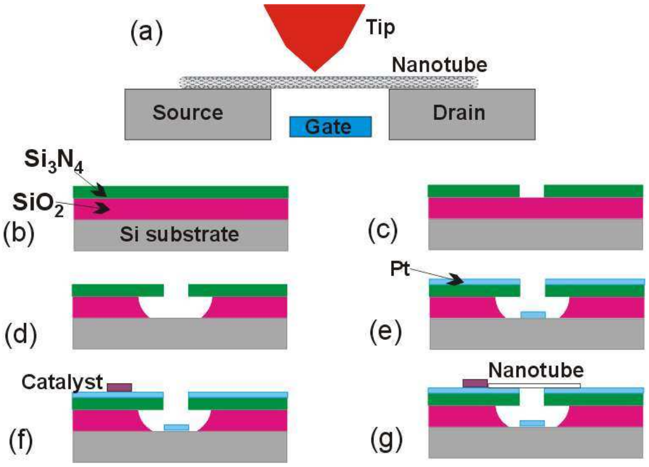

FIG. 1: (Color online) (a) Diagram of suspended nanotube structure for combined electron transport and STM studies. (b)-(g) Schematic of the fabrication process. (b) Starting substrate: Si with 500 nm thermally grown SiO_2 and 100 nm Si_3N_4. (c) Patterning and dry etching of trenches in Si_3N_4 layer. (d) Wet etching of SiO_2. (e) Evaporation of Pt (with 1 nm Ti as sticking layer) (f) Patterning and catalyst deposition. (g) After CVD growth, nanotubes are suspended over the trenches.

We choose Pt as the material for the conducting substrate. It is a noble metal which does not develop oxides in air, and is therefore suitable for imaging with STM. The melting point of Pt is 1772 °C, high enough to be compatible with the CVD process. In addition, it does not form hydrides at elevated temperatures[10] (the CVD process takes place in a hydrogen rich environment). The Pt-carbon phase diagram shows a eutectic alloying temperature at 1705±13 °C,[11] much higher than the CVD temperature. Consequently the presence of Pt does not interfere with the carbon nanotube growth.[12,13]

Our process starts with heavily doped p++ Si substrates with a 500 nm thermally grown oxide and 100 nm of Si_3N_4 on top (Fig 1(b)). Trenches in Si_3N_4 are opened by electron beam lithography (EBL) and anisotropic reactive ion etching with CHF_3 and O_2. Subsequently the resist is removed by acetone and the surface is cleaned by O_2 plasma (Fig 1(c)). An isotropic wet etch (Buffered HF) deepens the trench into the SiO_2 and creates an undercut (Fig 1(d)). This is followed by direct electron-beam evaporation of Pt over the whole substrate (Fig 1(e)), with 1 nm Ti as sticking layer. The undercut prevents the metal on the top from contacting the bottom. The Pt at the bottom of the trench, which forms PtSi after heating, is used as the gate electrode[14]. The positions for the catalyst are defined by EBL, and an alumina-supported iron catalyst is deposited on the substrate followed by lift-off in acetone[15] (Fig 1(f)). As a final step, nanotubes are grown by CVD at 800 °C (Fig 1(g)). The synthesis is carried out in a 1 inch diameter tube furnace under the flow of 910 mL/min of CH_4, 700 mL/min of H_2 and 40 mL/min of C_2H_4[16] for 5 minutes.

We have found that the final Pt surface depends very sensitively on trace amounts of O_2 present during the CVD process. The CVD synthesis takes place at 800 °C. When heating up and cooling down the reactor, a constant flow of H_2 (purity 99.999%) is applied. This step is crucial to obtain the desired trench structure for STM imaging. Fig 2(a) displays the result when Ar (purity 99.996%) instead of H_2 was used during heating up. Particles with crystalline facets can be seen decorating the edge of the trenches. These particles appear even when using a substrate without catalyst, and we conclude that they are Pt crystallites. It has been recognized in electrochemical studies that the oxidizing-reducing cycle leads to Pt surface reconstruction.[17] This was attributed to the fact that the oxidized Pt species diffuses across the surface more easily. Presumably in our case, Pt atoms are oxidized by the trace amount of O_2 (<10 ppm[18]) in the Ar and accumulate along the trench edges. Later during the CVD process they are reduced again in the H_2 rich environment. This leads to the faceted Pt particles decorating the trenches. In contrast, when H_2 is used during the heating up, it reduces the O_2 impurities, therefore significantly lessening the effect as shown in Fig 2(b). In order to even further reduce exposure to O_2, we flush the system at room temperature with H_2 for 20 min. As a result, the Pt migration is effectively eliminated (Fig 2(f)).

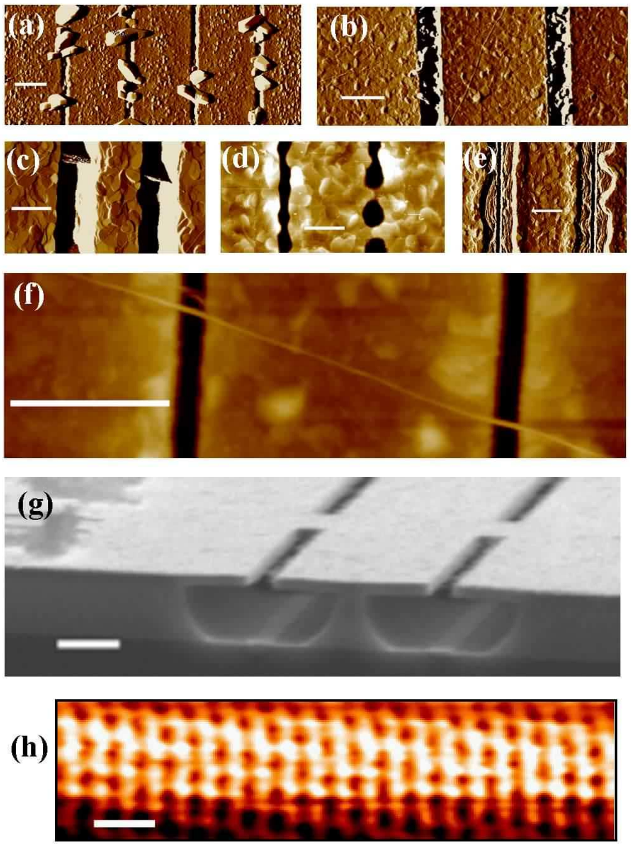

FIG. 2: (Color online) (a) AFM image of faceted Pt particles decorating the trench edges when heating the substrate in Ar. (b) AFM image of the device when H_2 is used instead of Ar but there is still a trace amount O_2 in the system. (c)-(e) AFM images showing trench widening and corrugation due to the heating. (f) AFM image of the result using the fast heating method. (g) cross-sectional SEM image of the final structure. (h) STM atomic resolution topography image on a suspended part of a SWCNT. The image is taken with a sample voltage of -0.1 V and a feedback current of 300 pA. Scale bars: (a)-(g): 500 nm, (h): 5 Å

Fig 2(c) - (e) display another issue we encounter during sample fabrication, i.e, the trenches become distorted after CVD synthesis. The effect becomes more severe when the thickness of the Pt film decreases. The Pt in Fig 2(c) is 100 nm thick and the trenches are 300 nm wide before the CVD. After the high temperature they appear to have become ∼ 450 nm wide. Although the trenches are widened, the edges are still straight and sharp. When the thickness of the Pt is decreased to 50 nm, the edges of the trenches become noticeably rougher as shown in Fig 2(d). Occasionally, this also causes short-circuiting of the two sides of the trench. When the Pt film thickness is reduced to 20 nm, the widening effect becomes universal. Fig 2(e) displays the edges of such a thin Pt film retracting away from 30 nm wide trenches. As suggested by this figure, this effect is probably due to the surface tension between the Pt film and the substrate at the edge of the trench, causing the Pt to be dragged away. The migration of the Pt film causes a severe problem for the integrity of the trench structure.

In order to prevent the degradation of devices, we adopted a fast heating/cooling technique.[19] The furnace was first heated up to the target temperature (800 °C) without the substrate. Once the temperature became stable, the desired gases were switched on and the substrate was quickly brought to the center of the furnace. After CVD synthesis for 5 min, the substrate was immediately brought out of the high temperature region. In this way the duration of substrate heating and the deformation of the Pt film were minimized. Fig 2(f) is a representative AFM image of the devices fabricated by this fast heating/cooling technique. Fig 2(g) is a cross-sectional SEM image of the device after CVD. Fig 2(h) presents a STM topography image of an individual metallic SWCNT suspended across a 200 nm trench demonstrating atomic resolution.

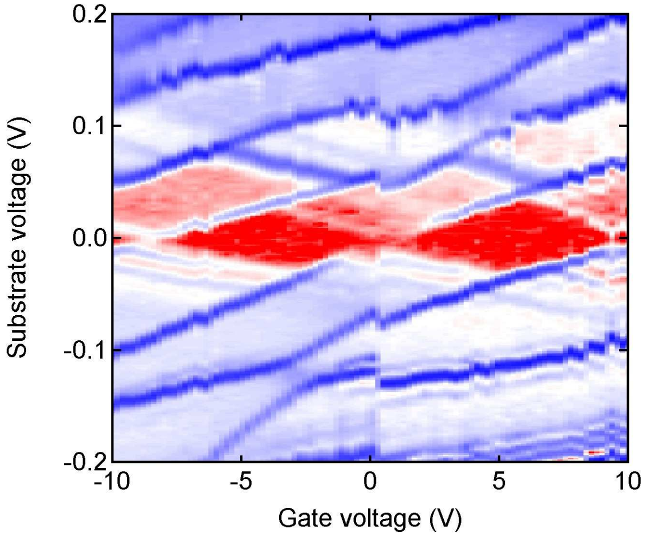

FIG. 3: (Color) Logarithm of differential conductance as a function of substrate and gate voltage for the nanotube in Fig 2(h) suspended over a 200 nm wide trench. The STM tip is held at a fixed location above the suspended portion of the SWCNT, with a setpoint current of 500 pA at a substrate voltage of -0.5 V with respect to the tip. Red corresponds to low values and blue corresponds to high values.

In order to demonstrate the potential of these devices, we present gated STM measurements. Our previous studies on non-gated nanotubes showed that the suspended parts of the nanotubes tend to form quantum dots and that Coulomb peaks are observed in the differential conductance dI/dV.[8] With the metal electrode at the bottom of the trench as a gate, the single-electron-charging behavior can be investigated in full detail. For the same nanotube imaged in Fig 2(h), we have performed tunneling spectroscopy measurements as a function of gate voltage. We used the STM tip as the source, the substrate as the drain, and the bottom electrode as the gate. The measurements were performed by adding a small ac voltage to the substrate voltage and using lockin detection at a temperature of 5 K.

The measured dI/dV as a function of sample and gate voltage is plotted in Fig. 3. It shows the characteristics of a typical Coulomb diamond plot.[20] Near zero substrate voltage, there are diamond shaped regions where the current is blocked and at higher voltages there are peaks associated with adding additional electrons to the SWCNT. Single-electron tunneling is observed with a Coulomb charging energy of about 40 meV. The periodicity of the diamonds and the lack of additional peaks implies that we are probing a single quantum dot. We do not see any evidence for multiple quantum dots in series or parallel such as, for example, induced by defects in the SWCNT. The ability to access the full Coulomb diamond plot allows us to unambiguously identify the origin of all the peaks in the differential conductance. The peaks sloping from the bottom left to the top right of the image are due to the Fermi energy of the substrate lining up with a state on the SWCNT. The peaks running from the top left to the bottom right are due to the Fermi energy of the tip lining up with states in the SWCNT. Excitations lines can be observed parallel to the edges of the Coulomb diamonds, and side peaks due to phonon-assisted tunnelling[9] are also visible.

The addition of the gate electrode allows the values of the capacitances in our device to be determined. From the slope of the edges of the Coulomb diamonds we can derive the capacitances: $C_{tip} \approx 1.8$ aF, $C_{substrate} \approx 2.5$ aF. The width of the diamond in gate voltage gives the value for $C_{gate} \approx 0.018$ aF. These values are in good agreement with a numerical simulation, where the tip is modelled as a 150 nm radius sphere. Experimentally, we find that the value of $C_{substrate}$ can vary between 1 and 10 aF depending on the extent of the quantum dot over the Pt substrate. The small SWCNT-substrate capacitance and hence large charging energy implies that the quantum dot does not extend very far over the Pt substrate. The gate coupling is relatively weak in this structure because of the presence of the Pt substrate and the STM tip. These large metal surfaces act to shield the gate from the SWCNT reducing its coupling.

In summary, we have incorporated a gate electrode into devices for STM studies of SWCNTs. Coulomb diamond plots were obtained using STM with simultaneous atomic-resolution imaging capability. With proper design, the metal on the two sides of the trench can be isolated and function as independent source and drain electrodes of the nanotube device. Combining transport measurements with STM studies of suspended SWCNTs opens many opportunities for further studying the electronic and mechanical properties of nanotubes.

The authors would like to thank FOM and NWO for funding, and A. Hassanien and J.-O Lee who were involved in earlier stages of this work.

---

[*] Electronic mail: dekker@mb.tn.tudelft.nl

[1] S. Iijima, Nature (London) **354**, 56 (1991).
[2] M.S. Dresselhaus, G. Dresselhaus, and P. Avouris *Carbon Nanotubes: Synthesis, Structure, Properties, and Applica-*

tions, (Springer, Berlin, 2001).

[3] C. Dekker, Phys. Today **52**, 22 (1999).

[4] P.L. McEuen, Nature (London) **393**, 15 (1998).

[5] J.W.G. Wildoer, L.C. Venema, A.G. Rinzler, R.E. Smalley, and C. Dekker, Nature (London) **391**, 59 (1998).

[6] T.W. Odom, J.L. Huang, P. Kim, and C.M. Lieber, Nature (London) **391**, 62 (1998).

[7] L. Gurevich, L. Canali, and L.P. Kouwenhoven, Appl. Phys. Lett. **76**, 384 (2000).

[8] B.J. LeRoy, S.G. Lemay, J. Kong, C. Dekker, Appl. Phys Lett. **84**, 4280 (2004).

[9] B.J. LeRoy, S.G. Lemay, J. Kong, C. Dekker, Nature (London) **432**, 371 (2004).

[10] N.R. Franklin, Q. Wang, T.W. Tombler, A. Javey, M. Shim, and H. Dai, Appl. Phys. Lett. **81**, 913 (2002).

[11] W.G. Moffatt, *The Handbook of binary phase diagrams*, Vol II, (Gemium Publishing Corporation, 1984).

[12] H.B. Peng, T.G. Ristroph, G.M. Schurmann, G.M. King, J. Yoon, V. Narayanamurti and J.A. Golovchenko, Appl. Phys. Lett. **83**, 4238 (2003).

[13] J. Cao, Q. Wang, D. Wang, and H. Dai, Small **1**, 138 (2005).

[14] Alternatively, we can etch the SiO_2 halfway, leaving the Pt inside the trench floating. The p++ Si then serves as the gate.

[15] J. Kong, H.T. Soh, A.M. Cassell, C.F. Quate, H. Dai, Nature (London) **395**, 878 (1998).

[16] N.R. Franklin, Y. Li, R.J. Chen, A. Javey, and H. Dai, Appl. Phys. Lett. **79**, 4571 (2001).

[17] K. Itaya, S. Sugawara, and K. Sashikata, J. Vac. Sci. Technol. A **8**, 515 (1990).

[18] Gas analysis from Hoek Loos B.V, the Netherlands.

[19] S.M. Huang, M. Woodson, R. Smalley, J. Liu, Nano Lett. **4**, 1025 (2004).

[20] H. Grabert and M.H. Devoret, *Single Charge Tunneling* (Plenum, New York, 1992).